



HAL
open science

Influence of Sawtooth Patterns on the Detection Properties of Quantum Well Infrared Photodetectors

Emmanuel Lhuillier, Vincent Gueriaux, Virginie Trinite, Mathieu Carras

► **To cite this version:**

Emmanuel Lhuillier, Vincent Gueriaux, Virginie Trinite, Mathieu Carras. Influence of Sawtooth Patterns on the Detection Properties of Quantum Well Infrared Photodetectors. *IEEE Journal of Quantum Electronics*, 2012, 48 (5), pp.665 - 668. 10.1109/JQE.2012.2189373 . hal-01438664

HAL Id: hal-01438664

<https://hal.science/hal-01438664>

Submitted on 23 Jan 2017

HAL is a multi-disciplinary open access archive for the deposit and dissemination of scientific research documents, whether they are published or not. The documents may come from teaching and research institutions in France or abroad, or from public or private research centers.

L'archive ouverte pluridisciplinaire **HAL**, est destinée au dépôt et à la diffusion de documents scientifiques de niveau recherche, publiés ou non, émanant des établissements d'enseignement et de recherche français ou étrangers, des laboratoires publics ou privés.

Influence of sawtooth patterns on the detection properties of Quantum Well Infrared Photodetectors.

Emmanuel Lhuillier, Vincent Guériaux, Virginie Trinité and Mathieu Carras

Abstract—Sawtooth patterns in the $I(V)$ curves of superlattices result from the bistability induced by the negative differential resistance of the local $J(F)$ curve. This behavior has been extensively studied in weakly coupled superlattices from a transport point of view. In this paper, we show that the sawtooth pattern not only affects the dark current but also the noise and responsivity properties of a quantum well infrared photodetector. The impact on the imaging properties of the detector is also quantified.

Index Terms— QWIP, sawtooth, electric field domain, noise, response

I. INTRODUCTION

Superlattices, made from III-V heterostructures, gave birth to a large range of new transport phenomena [1]. In particular, negative differential resistance [2-3] (NDR) comes out in weakly coupled structures through the presence of sawtooth patterns in the device $I-V$ curve. This behavior has been extensively studied both experimentally [3-4] and theoretically [5-6]. These oscillations can be used for the realization of oscillators in the GHz range [7] or can lead to a chaotic evolution [8]. The interested reader can refer to the review of Wacker's [9] or Bonilla and Grahn's [10] review for much more details.

These superlattices have been used for infrared photodetection and are identified as quantum well infrared photodetectors (QWIP). When QWIP are dedicated to very low photon flux detection it may be interesting to operate them at low temperature where the dark current is limited by the tunneling process through the inter-well barrier. In this case, QWIP behave as an ultra-weakly coupled superlattice (i.e. mini-bandwidth is in the neV to μ eV range). Observation of sawtooth patterns in the dark $I-V$ curves of QWIP is already well established [11]. Here we investigate the effect of the sawtooth patterns on the response and noise of the QWIP. Finally we draw conclusions on the ability of QWIP to operate in this regime.

EL was graduate student at ONERA, centre de Palaiseau, Chemin de la Hunière - FR 91761 Palaiseau cedex, France. He is now post doc at the James Franck institute, university of Chicago, 929 E 57th street, 60637 Chicago, IL USA

VG, CT and MC are research scientists at III-V Lab, Campus de Polytechnique, 1 Avenue A. Fresnel, 91761 Palaiseau cedex, France.

II. EXPERIMENTAL SECTION

GaAs/Al_xGa_{1-x}As QWIP have been grown by molecular beam epitaxy. Sample S₁ (S₂) which will be studied in this paper has 4.8nm wells and 20nm (15nm) barriers. Barriers include 26% aluminum. The forty periods are silicon doped, at a $2 \times 10^{11} \text{cm}^{-2}$ level, into the well. The peak wavelength of the structure is 8.4 μm . The structure is then processed into mesas. We address also the effect of changing the detection wavelength on the sawtooth pattern with a 17 μm peak wavelength devices S₃ and S₄ (8nm well, 40nm barrier, 12,5% of aluminum). The samples differ by the doping level: $2 \times 10^{11} \text{cm}^{-2}$ for S₃ and $4 \times 10^{11} \text{cm}^{-2}$ for S₄.

For characterization, the samples were put on the cold finger of a helium cryostat. $I-V$ curves are measured at 23K, while noise and responsivity are measured at liquid nitrogen temperature. All the acquisitions of the $I-V$ curves have been conducted with the following process. After switching bias, we let the system rest for 1s, to reach steady state, then average three acquisitions of the current. Thus we perform only steady state measurements. Current measurements were performed using a Keithley 6487 pico-ammeter. $I-V$ curves under illumination were acquired while the detector was exposed to 50°C blackbody radiation. The spectral measurements were made with a Nicolet Avatar 360 FTIR spectrometer (with a 0.64cm.s^{-1} modulation speed and averaged over 128 spectra corresponding to 3 minutes of acquisition). The noise measurements were obtained after magnification (using pre-amplifier Princeton Applied Research model 181 and an amplifier Stanford research system SR560) via a Stanford SR760 spectrum analyzer.

III. DISCUSSION

A. Effect on the dark transport

The dark $I-V$ curve of the sample S₁ is shown in figure 1. We can split this curve into three different zones. An initial, mostly ohmic growth, in the 0 to 0.5V range of bias, includes a large NDR, which is attributed to a contact effect. Similar effect has been observed in tunnel resonant diode [12]. Then there is a plateau between 0.7V and 4V, with sawtooth patterns. The inset A₁ is zoomed in on this plateau area. Above 4V, the $I-V$ restarts to rise monotonically. The number of sawtooths is close to the number of periods, but stays lower by two or three units

depending on the growth. This discrepancy can be explained by including growth irregularity [13-14] or edge effect. Briefly, the origin of the sawtooth pattern can be understood by the combination of three equations, describing charge conservation, the Poisson equation and the local I - V or J - F curve. For modeling we use the equation given by Amann *et al.* in reference [15]. The NDR in the local (i.e. over a single barrier) J - F curve results in two electric fields giving the same current. By increasing the bias, a well can switch from the low electric field regime to the high electric field regime. This change comes with an excess or deficit of charge at the transition. Finally, the sawtooth results from this excess (or deficit) charge zone moving through the superlattice [15]. Changing the barrier size from 20 to 15 nm, we observe a change in the sub-pattern inside the sawtooth, compare insets A_1 and A_2 of figure 1. The presence of NDR in the sub pattern is not understood at the moment. The change of the current density level is well explained into a sequential tunneling approach [9] by the change of coupling between adjacent well. Sawtooth patterns are observed on a large range of QWIP detecting at very different wavelength, with a $17\mu\text{m}$ peak wavelength device S_3 also exhibiting them; see figure 1 inset B_1 . Finally, we observe that by increasing the doping by a factor of two in sample S_4 relative to S_3 , the sawtooth pattern disappears, see inset B_2 of figure 1. We attribute this lack of sawtooth pattern in the highly doped device to the reduction of the peak-valley ratio in the local J - F curve due to the increase of the valley current. In fact the valley current is dominating by non-resonant term [9, 12] and higher impurity content can explain a greater scattering rate and current.

B. Effect on noise density

Not only does the sawtooth pattern affect the dark current, but also the noise and the responsivity. Noise current spectral density is plotted on figure 2 for sample S_2 . The noise spectral density presented here consists of an average of 1024 spectra around 8kHz. Between each change of bias we wait for the system to reach the stationary state. The current is plotted as well for comparison. The noise exhibits the sawtooth pattern for the same bias as the current. On the noise density curve, we observe some noise excess [16] (sharp peak) at the transition between two sawtooth branches. This could be due to fluctuations of the charge distribution between the two configurations just at the transition bias. Apart from these sharp peaks, the sample exhibits a white noise behavior in the 1kHz to 100kHz range.

The usual model for noise in QWIP is the generation-recombination (GR) noise associated with tunneling transport, which is a shot noise [17-18], whose magnitude is expected to follow the law $NSD_{GR} = \sqrt{4egI}$, where e is the elementary charge, g the noise gain, and I the current through the pixel. Beck¹⁷ has predicted that in the case where tunneling transport prevails, the gain can be written as $g = \frac{1}{2N}$ where N is the number of periods. This leads to the final expression for the

shot noise spectral density $NSD_{Shot} = \sqrt{\frac{2eI}{N}}$. This

expression is equivalent to the shot noise ($\sqrt{2eI}$) of N uncorrelated wells in series. The presence of an additional thermal noise may also be investigated, in which case the Johnson noise has the following expression

$$NSD_{Johnson} = \sqrt{\frac{4k_b T}{R_d}}$$

where R_d is the differential resistance

which can be evaluated by differentiating the I - V curve. The plot of the Johnson and shot noise as a function of bias is given in figure 2. These modeled noises effectively present sawtooth patterns and sharp peaks at the transitions between the latter. Nevertheless, and even by adding those two sources of noise, the modeled noise level is lower than the experimental noise by at least a factor three. This noise enhancement comes from an additional source of noise. From the literature it may result from a coherent effect over more than one period [18] or from a recharging time due to the domain field formation [19].

C. Effect on photo-response

Finally, we study the effects of the sawtooth pattern on the responsivity. We operate the QWIP in a regime of photon flux where the dark current is still prevailing. Photocurrent has already been used as a probe for electric field domains in superlattices [20], but no work is focused on the detection properties. Indeed, as with the dark current and noise, the responsivity also shows the sawtooth patterns. The integrated response of the spectrum ($R_{int} = \int_{\Delta\lambda} R(\lambda, V) \cdot d\lambda$ with R the

spectral response) is plotted in figure 3 (a) for sample S_1 . The curve has a sawtooth pattern, but with a reverse slope compared to the dark current. Due to this reverse slope, the detectivity value at the bottom of a current sawtooth is higher than the detectivity value at the top of the previous one. We also observe the rise of the base line with the bias which is due to the fact that the number of periods in the high electric field domain increases; and in a higher electric field the quantum well has a higher extraction probability for the photo-excited carriers. The change of sawtooth pattern is also concomitant with a change of the spectral response, see figure 3 (b). At a bias where the current jumps, the high energy part of the spectrum is reduced, but we have no clear explanation for this feature.

To model this response we consider the response of the detector as the product of the gain of the structure (taken constant and equal to 0.25), the probability p_e of emission of the well given by the WKB approximation, and the absorption α of each well

$$R(\lambda, F) = \frac{e\lambda}{hc} \cdot g_{photo} \cdot \sum_{well} p_e(\lambda, F)[i] \cdot \alpha(\lambda, F)[i] \quad (1),$$

with e the elementary charge, λ the peak wavelength, h the Planck's constant and c the speed of light. Following reference [21], the absorption of a single well is given by:

$$\alpha(E_{ph}, F) = n[i] \frac{e^2}{\hbar \cdot \epsilon_0 \cdot c \cdot n_{opt}} \cdot E_{ph} \cdot \left| \langle \Psi_0 | Z | \Psi_1 \rangle \right|^2 \cdot \left| \frac{E_{EM}(z)}{E_{EM}(0)} \right|^2 \frac{1}{\Gamma} \frac{1}{1 + \left(\frac{E_{ph} - E_{12}}{\Gamma} \right)^2} \quad (2).$$

With n the charge of well $[i]$, n_{opt} is the optical index of refraction (taken equal to 3.3 in GaAs), Z the dipole element

evaluated using a kp code. $\left| \frac{E_{EM}(z)}{E_{EM}(0)} \right|$ is the ratio of the

absorbable electromagnetic field over the incident electromagnetic field, obtained from an exponential fit of the electromagnetic field profile calculated by a finite difference method [22], $E_{12} = E_2 - E_1$ the transition energy between the ground state and the first excited state, and $\Gamma = 5$ meV is the full width at half maximum of the photonic transition which is expected to have a lorentzian shape. Results of the simulation are given in the inset of figure 3 (a). We are able to reproduce both the sawtooth pattern of the dark current and the photoresponse, with their opposed slopes. The reverse slope results from the fact that the response is driven by the product $p_e(\lambda, F)[i] \times n_m[i]$. This product is almost constant over the structure except over the well at the boundary of the electric field domains. In this well the product decreases when the bias rises. However such a simple model leads to discrepancies on the absolute values of photocurrent.

It is interesting to note the effect of the sawtooth pattern on the detectivity. Transitions between different sawtooth patterns occur over a bias change of less than $200 \mu\text{V}$, which is smaller than the bias uniformity of most read out circuits. Thus, different pixels of a focal plane array may operate under different electric field distributions. Under low photon flux the resulting variation of detectivity can be as high as 30% for a flux of $10^{15} \text{ photons} \cdot \text{s}^{-1} \cdot \text{cm}^{-2}$. These values give the upper limit for the non-uniformity of the focal plane array in this regime.

IV. CONCLUSION

To conclude, we have demonstrated that sawtooth patterns are seen not only in the current but also the noise and responsivity of QWIP when the transport is tunnelling limited in the presence of electric field domains. Thus, noise and photoresponse can be used as a probe in multistable or chaotic systems, in addition to regular dark transport measurements. Moreover we have shown that the presence of these sawtooth patterns affects the imaging performance in the low photon flux regime. Different strategies may be followed to avoid such sawtooth patterns, including increasing the doping level or the barrier length, increasing the operating temperature to reach the thermally activated regime, or operating under large enough photon flux to suppress the dark current effects.

ACKNOWLEDGMENT

The authors want to thank A. Nedelcu, E. Costard and P. Bois for their support and fruitful discussions for the realization of this work. We are also very grateful to B. Vinter, S. Keuleyan and R. Shah for their careful reading of the manuscript

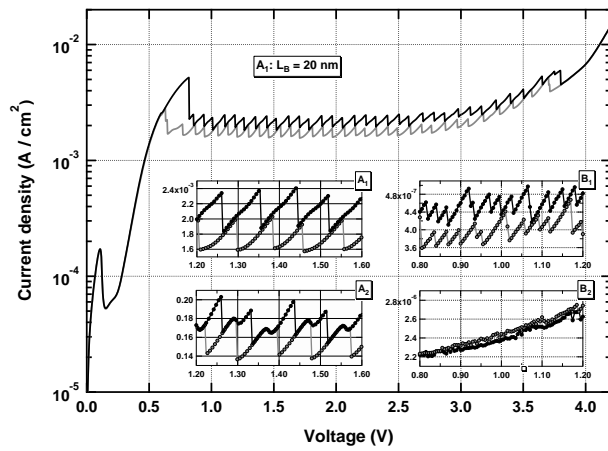


Figure 1: Dark I - V curve at 23K of sample S_1 . The inset A_1 is zoomed in on the range of 1.2V to 1.6V bias. The inset A_2 is for sample S_2 which has a thinner barrier. The inset B_1 is for sample S_3 which has a $17\mu\text{m}$ peak response. The inset B_2 is for sample S_4 which has twice higher doping.

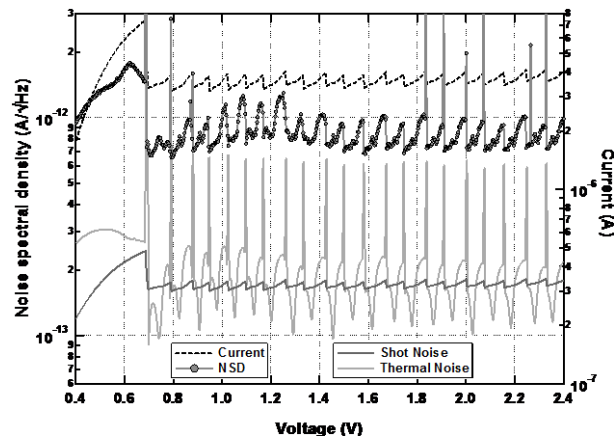


Figure 2: Dark current and current noise spectral density as a function of the applied bias for sample S_2 at 77K. Shot noise and thermal noise analytically evaluated from the current value are also plotted as dotted line for comparison with the experimental value.

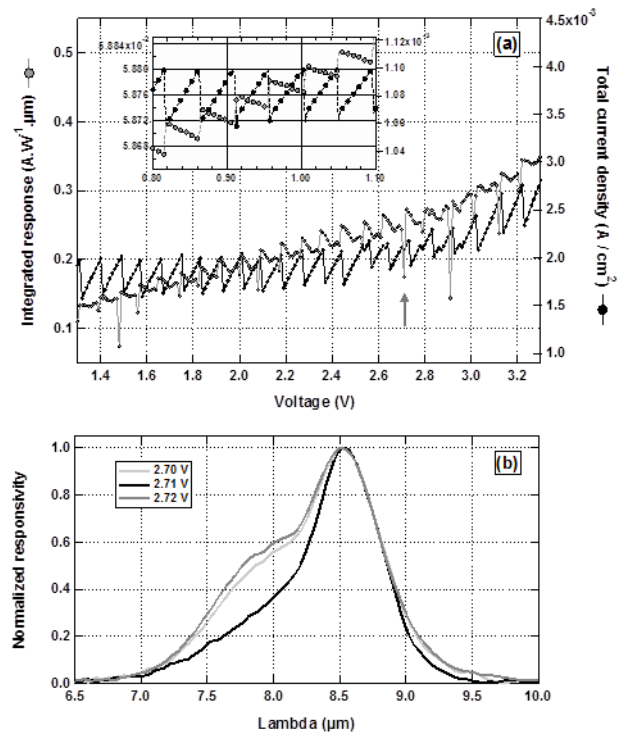


Figure 3: (a) integrated response (left) and current density (right) as a function of the applied voltage, for sample S_1 at 77 K. The inset shows the simulation of the same properties. (b) Normalized spectral response for three different voltages around a transition between sawtooth patterns.

Emmanuel Lhuillier did his college at ESPCI (Paris France) and then followed a graduate program from Ecole Polytechnique made at ONERA on electronic transport in superlattice used as infrared photodetector. He is currently in post doc at the university of Chicago where he studies the mid infrared detection using colloidal quantum dots.

Vincent Guériaux did his college at IFIPS and then a PhD program at Alcatel thales III-V Lab on quantum well infrared photodetectors from mid-infrared to long wavelength. He is currently working for Thales optronic.

After her college at Ecole Centrale Paris, Virginie Trinité did a graduate program at Ecole Polytechnique on the theoretical study of titanium phase. She then joins the simulation group of Alcatel thales III-V Lab, where her research focus the properties of III-V heterostructures.

Mathieu Carras, Mathieu Carras is a former student of Ecole Centrale and he then made its PhD at Thales R&T on quantum well infrared detector. He currently leads the quantum cascade department of Alcatel thales III-V Lab.

REFERENCES

- [1] R.F. Kazarinov and R.A. Suris, "Electrical and electromagnetic properties of semiconductors with a superlattice", *Sov. Phys. Semicond* **6**, 120 (1972).
- [2] L. Esaki and L. L. Chang, "New Transport Phenomenon in a Semiconductor "Superlattice"", *Phys. Rev. Lett.* **33**, 495 (1974).
- [3] B.F. Levine, K.K. Choi, C.G. Betha, J. Walker, R.J. Malik, "New 10 μm infrared detector using intersubband absorption in resonant tunneling GaAlAs superlattices", *Appl. Phys. Lett.* **50**, 1092 (1987).
- [4] K. K. Choi, B. F. Levine, R. J. Malik, J. Walker, and C. G. Bethea, "Periodic negative conductance by sequential resonant tunneling through an expanding high-field superlattice domain", *Phys. Rev. B* **35**, 4172 (1987).
- [5] L. L. Bonilla, J. Galán, J. A. Cuesta, F. C. Martínez, and J. M. Molera, «Dynamics of electric-field domains and oscillations of the photocurrent in a simple superlattice model», *Phys. Rev. B* **50**, 8644 (1994)
- [6] A. Wacker, M. Moscoso, M. Kindelan and L. L. Bonilla, "Current-voltage characteristic and stability in resonant-tunneling n-doped semiconductor superlattices", *Phys. Rev. B* **55**, 2466 (1996).
- [7] J. Kastrup, R. Hey, K. H. Ploog, H. T. Grahn, L. L. Bonilla, M. Kindelan, M. Moscoso, A. Wacker and J. Galan, "Electrically tunable GHz oscillations in doped GaAs-AlAs superlattices", *Phys. Rev. B* **55**, 2476 (1996).
- [8] O. M. Bulashenko and L. L. Bonilla, "Chaos in resonant-tunneling superlattices", *Phys. Rev. B* **52**, 7849 (1995).
- [9] A. Wacker, "Semiconductor *Superlattices*: A model system for nonlinear transport", *Phys. Rep.* **357**, 1 (2002).
- [10] L. L. Bonilla and H. T. Grahn, "Non-linear dynamics of semiconductor superlattices", *Rep. Prog. Phys.* **68**, 577 (2005).
- [11] K.-K. Choi, B. F. Levine, C. G. Bethea, J. Walker, and R. J. Malik, "Multiple quantum well 10 μm GaAs/Al_xGa_{1-x}As infrared detector with improved responsivity", *Appl. Phys. Lett.* **50**, 1814 (1987).
- [12] F. Chevoir, B. Vinter, « Scattering-assisted tunneling in double-barrier diodes: Scattering rates and valley current", *Phys. Rev. B* **47**, 7260 (1993).
- [13] G. Schwarz, A. Wacker, F. Prengel, E. Scholl, J. Kastrup, H.T. Grahn and K. Ploog, „The influence of imperfections and weak disorder on domain formation superlattices Semicond“, *Sci. Technol.* **11**, 475 (1996).
- [14] A. Wacker, G. Schwarz, F. Prengel, E. Scholl, J. Kastrup and H.T. Grahn, "Probing growth-related disorder by high-field transport in semiconductor superlattices", *Phys. Rev. B* **52**, 13788 (1995).
- [15] A. Aman, A Wacker, L.L. Bonilla and E Scholl, "Dynamic scenarios of multistable switching in semiconductor superlattices", *Phys. Rev. E* **63**, 066207 (2001).
- [16] M. Gattobigio, G. Iannaccone and M. Macucci, "Enhanced Shot Noise in Resonant Tunneling: Theory and Experiment", *Phys. Rev. Lett.* **80**, 1054 (1998).
- [17] W. A. Beck, "Photoconductive gain and generation-recombination noise in multiple-quantum-well infrared detectors", *Appl. Phys. Lett.* **63**, 3589 (1993).
- [18] Y.P. Li, A. Zaslavsky, D. C. Tsui, M. Santos, and M. Shayegan, "Noise characteristics of double-barrier resonant-tunneling structures below 10 kHz", *Phys. Rev. B* **41**, 8388 (1990).
- [19] R. Rehm, H. Schneider, M. Walther and P. Koidl, "Influence of the recharging process on the dark current noise in quantum-well infrared photodetectors", *Appl. Phys. Lett.* **80**, 862 (2002).
- [20] S. H. Kwok, T. B. Norris, L. L. Bonilla, J. Galán, J. A. Cuesta, F. C. Martínez, and J. M. Molera, H. T. Grahn and K. Ploog and R. Merlin, "Domain-wall kinetics and tunneling-induced instabilities in superlattices", *Phys. Rev. B* **51**, 10171 (1995).
- [21] E. Rosencher and B. Vinter, in *Optoelectronics (Cambridge University Press, Cambridge, 2002)*.
- [22] A. De Rossi, E. Costard, N. Guérineau and S. Rommeluère, "Effect of finite pixel size on optical coupling in QWIP's", *Infrared Phys. Techn.* **44**, 325 (2003).